



On the transient dynamic antiplane contact problem in the presence of dry friction and slip

B. Gurrutxaga-Lerma^{a,b,*}

^aTrinity College Cambridge, University of Cambridge, Cambridge CB2 1TQ, UK

^bDepartment of Engineering, University of Cambridge, Trumpington Street, Cambridge CB2 1PZ, UK



ARTICLE INFO

Article history:

Received 6 September 2018

Revised 10 February 2019

Available online 11 April 2019

Keywords:

Elastodynamic

Contact

Antiplane

Stick

Slip

ABSTRACT

This article models the elastodynamic transient contact between two elastically similar half planes under antiplane loading and in the presence of friction. Contact is maintained along the positive real line under the presence of a certain remote contact pressure. An antiplane shear load is applied, which entails interfacial shear traction that opposes the frictional force entailed by the contact pressure. In order to balance the surface tractions, the surface must be allowed to slip. We derive the closed form solution of the interfacial traction due to a general antiplanar displacement distribution using a variant of the Wiener-Hopf technique. We also find closed-form expressions for the interfacial shear traction due to this remote antiplane load. In combination with the frictional force, this leads to an integral equation the solution to which is the distribution of relative slip. We quantify both this and the magnitude of the interfacial shear tractions under diverse loading, showing that transient loading leads to partial reverse slip of the contact surfaces. We show that the reverse slip tends to vanish over time, and that it is ameliorated if the friction coefficient is reduced.

© 2019 Elsevier Ltd. All rights reserved.

1. Introduction

This article discusses the elementary solutions governing the antiplane, elastodynamic contact between two elastically similar bodies in the presence of friction and slip. Elastodynamic contact is of particular relevance at high strain rates (Meyers, 1994), under shock (Abou-Sayed et al., 1976; Doyle, 1987) or ramp loading (Brown et al., 2013), and generally in the description of contact problems where the representative time and lengthscales are comparable to the relevant speeds of sound of the material, such as those that may for instance be encountered in turbine shaft bearings (Khonsari and Booser, 2008; Hirani et al., 1999; Schwingshackl et al., 2012), where the loading rates quickly approach the material's speed of sound; in joints in flexible structures, where the speed of sound at the joint is much slower than that at the structure itself (Gaul and Lenz, 1997; Gaul and Nitsche, 2001); or in brakes, where dynamic contact is involved in frictional induced vibrations (Wayne, 2000; Butlin and Woodhouse, 2009) which are also of relevance in structural mechanics (Duffour and Woodhouse, 2007, 2004; Woodhouse and Duffour, 2004). In such situations, the conventional contact equations ought to account for the inertial

forces of the material, and the problem, formerly parabolic, becomes time dependent and hyperbolic. This entails a number of theoretical complications which means that dynamic contact has in the past received less attention than its static counterpart.

A considerable number of the dynamic contact problems that have been studied in the past involve moving contact problems in the absence of friction (Barber, 2018). These problems can be greatly simplified under the assumption that the contact surfaces slide at constant speed, because in those cases the fundamental solutions become self-similar (Eringen and Suhubi, 1975) (or, equivalently, homogeneous to degree zero in space and time (Freund, 1974)), so that the problem may be studied in the steady-state as a simple function of the sliding velocity. This approach has proven particularly useful in studying the role inertial forces may play in kinetic sliding contacts in plane strain, as done for instance by Galin (1961), Erigen and Suhubi, 1975, Craggs and Roberts (1967), Georgiadis and Barber (1993), or Brock (2002), amongst many others. This class of problems quickly stumbles upon some complications when exploring sliding motions above the Rayleigh wave speed and in the *transonic* regime, since the contact surface in those cases appears to be non-unique, and entails the presence of moving singularities (Barber, 2018). Such problems were recently clarified by Slepyan and Brun (2012), who offered a complete account of that nature of these singularities and how to regularise them in steady state contact problems of this kind.

* Corresponding author at: Trinity College Cambridge, University of Cambridge, CB2 1TQ Cambridge, UK.

E-mail address: bg374@cam.ac.uk

geophysical fault subjected to antiplanar loading, and is justified because the elastodynamic loads are expected to propagate away from the edge of the contact interface over very short periods of time. As is shown in Fig. 1, *ex hypothesi*¹, hereafter the contact interface is defined to be the positive half real line, i.e., the contact exists and has to be maintained only for $x > 0$, whilst for $x < 0$ the interfaces are free surfaces.

This contact is maintained by a certain remote load $P(x, t)$. Along the interface, this remote load induces a certain interfacial normal load $N(x, t)$, which in turn entails a frictional distributed force acting along the interface of the form $F_{\text{fric}}(x, t) = f \cdot N(x, t)$, where f is the friction coefficient. As a first approach, here we do not concern ourselves with the nature of such friction coefficient, and we assume the simple case of dry friction obeying Amonton's law. In more complete approaches one would consider circumstances where the frictional coefficient itself is a function of the interfacial shear slip (see for instance (Rice, 1993; Scholz, 1998)); in such situations, the problem would quickly become heavily non-linear. Such cases will be the subject of future work.

Here, the frictional force $F_{\text{fric}}(x, t)$ is balanced by a net interfacial shear traction $q(x, t)$, which we allow to be the result of two contributions:

1. That due to the interfacial shear traction $r(x, t)$ induced by a remote antiplane shear traction $R(x, t)$, which will be prescribed by us.
2. That due to slip, i.e., the interfacial shear traction $s(x, t)$ entailed by a certain, a priori unknown antiplane displacement distribution $w(x, t)$ which describes the relative slip between the two surfaces in contact. This slip is necessary to accommodate possible imbalances between the frictional and shear loads.

The elastodynamic approach mirrors the usual treatment of contact under the presence of friction and slip (Barber, 2018; Johnson, 1987; Nowell and Hills, 1987). In particular, we shall distinguish between regions of stick and slip. In slip regions we have

$$F_{\text{fric}}(x, t) = fN(x, t) = |q(x, t)| = |s(x, t) + r(x, t)| \quad (2.1)$$

with the condition that $\text{sign}(\partial_t u_z) = -\text{sign}(q(x, t))$ (q.v. Hills and Nowell (1994), p. 43). Hereafter this condition will be referred to as the 'kinematic contact condition', and its significance discussed in Section 6.

In stick regions, in turn

$$|q(x, t)| \leq fN(x, t) \quad (2.2)$$

subject to the additional kinematic condition that $\partial_t u_z = 0$. In the following, and for simplicity, we shall assume that $q(x, t)$ and $F_{\text{fric}}(x, t)$ are of the same sign and, accordingly, that the underlying slip is of opposite sign to the frictional traction.

The elastodynamic problems we ought to solve are therefore four:

1. We must find an expression for the interfacial shear traction $r(x, t)$ arising from the remote shear traction $R(x, t)$. This is Kostrov's problem, which has a well-known solution (see Kostrov, 1966; Achenbach, 1973).
2. We must find a mathematical expression for the interfacial shear traction $s(x, t)$ due to the relative slip displacement distribution $w(x, t)$ acting along the interface. This $w(x, t)$ is a priori unknown, and may or may not be compactly supported, albeit we expect it to be so over at least some finite region $x \in (0, a)$ (cf. Johnson, 1987; Nowell and Hills, 1987).
3. We must find an appropriate expression for $N(x, t)$.

4. The actual problem we are interested in solving is finding the slip displacement $w(x, t)$ arising from the force balance eqn. 2.1 between the frictional force and the two interfacial shear traction contributions. This will in principle entail an integral equation.

In the following, we give the general form of $s(x, t)$ and $r(x, t)$ under elastodynamic loading.

3. Interfacial shear traction due to remote antiplanar loading

Let $R(x, t)$ be some remote and arbitrary shear force acting in the antiplane z -direction over the system shown in Fig. 1. We wish to find the corresponding interfacial shear $r(x, t)$ traction acting along the contact interface ($x \in \mathbb{R}^+$).

The governing equation is (Achenbach, 1973):

$$\nabla^2 u_z(x, y, t) = b^2 \ddot{u}_z \quad (3.1)$$

where $u_z(x, y, t)$ is the out-of-plane (hereafter, antiplanar) displacement field component, which in antiplanar motion is assumed not to be dependent on z ; and where $b = \sqrt{\rho/\mu}$ is the transverse slowness of sound for ρ the material density and μ the shear modulus.

The boundary value problem concerns the geometry shown in Fig. 1. We require that the free surface $x < 0$ remains traction free under some remote loading $R(x, t)$. We model the reciprocal problem, whereby we negate $R(x, t)$ along the free surface, and require that the displacement along the contact interface vanish by symmetry. Thus,

$$\begin{aligned} \sigma_{yz}(x, 0, t) &= -R(x, t) & x \in \mathbb{R}^- \\ u_z(x, 0, t) &= 0 & x \in \mathbb{R}^+ \end{aligned} \quad (3.2)$$

What we wish to find is $r(x, t)$, the interfacial shear traction for $x \in \mathbb{R}^+$.

The solution to 3.1 when subjected to boundary conditions such as 3.2 can be expressed in terms of the representation theorem (q.v. Kennett, 1972; Udías, 2002) that relates the displacement field to a body force distribution via the system's Green's function (Aki and Richards, 2002). For antiplanar loading, this takes the form

$$u_z(x, y, t) = \int_{-\infty}^t dt' \int_{\mathbb{R} \times \mathbb{R}} dx' dy' G_{zz}(x - x', y - y', t - t') f_z(x', y', t') \quad (3.3)$$

where $G_{zz}(x, y, t) \equiv G_z(x, y, t)$ denotes the relevant antiplanar Green's function of the problem in question (Mura, 1982; Achenbach, 1973) (e.g., for an elastic half space, or for an infinite plane), and $f_z(x, y, t)$ any antiplanar force distribution acting on the system.

The solution procedure we briefly outline in the following relies on this representation theorem, and is due to Kostrov (1966), who applied it to the study of unsteady crack propagation of finite antiplane cracks. Achenbach (1973), Aki and Richards (2002), and Freund (1998), amongst others, reproduce variations of the derivation. As noted by Kostrov (1966), $r(x, t)$ has by construction support only for $x > 0$, and, again by construction, $R(x, t)$ has support only for $x < 0$. We can therefore write a global interfacial shear traction as $T(x, t) = -R(x, t) + r(x, t)$ acting along the whole interface (i.e., $x \in \mathbb{R}$ for $y = 0$). The first term, $R(x, t)$, is fixed and prescribed, and the displacements along $x \in \mathbb{R}^-$ can be arbitrary. However the displacements along $x \in \mathbb{R}^+$ must vanish. This means that $r(x, t)$ is the interfacial shear traction that ensures that the displacement field along $x \in \mathbb{R}^+$ cancels.

In considering $T(x, t)$, we are considering a distributed shear traction acting along the whole $y = 0$ abscissae line. The problem of solving the elastic fields resulting from the application of any such $T(x, t)$ over an elastic half space is Lamb's (antiplane) problem. The interfacial displacement field $u_z^T(x, 0, t)$ due to $T(x, t)$ can

¹ But without loss of generality owing to the translational invariance of the stress measure.

be obtained from $T(x, t)$ via the representation theorem:

$$u_z^T(x, 0, t) = \int_{\mathbb{R} \times \mathbb{R}} \int_0^t T(x', t') G_z(x - x', y - y', t - t') dt' d(x' \times y') = 0 \tag{3.4}$$

where $G_z(x, y, t)$ is the antiplane Green's function for an elastic half space, which is given by Achenbach (1973) and Freund (1998)

$$G_z(x, y, t) = -\frac{1}{\pi \mu} \frac{1}{\sqrt{t^2 - b^2 r^2}} H(t - br), \quad r = \sqrt{x^2 + y^2} \tag{3.5}$$

We then substitute $T(x, t) = -R(x, t) + r(x, t)$, with $R(x, t)$ known, on Eq. (3.4), leading to the following integral equation for $y = 0$:

$$\int_{\Gamma_1} \frac{R(x', t')}{\sqrt{(t - t')^2 - b^2(x - x')^2}} dt' dx' + \int_{\Gamma_2} \frac{t(x', t')}{\sqrt{(t - t')^2 - b^2(x - x')^2}} dt' dx' = 0 \tag{3.6}$$

The integration limits are found from the support imposed by the $H(t - br)$ functions, which define $\Gamma_1 = \{0, \infty\} \times \{0, t_s\}$ and $\Gamma_2 = \{-\infty, 0\} \times \{0, t_s\}$ with $t_s = \max(0, t - b|x - x'|)$. From that it follows that the equation above may be written as an integral equation of Abel type, the solution to which is given by Achenbach (1973)

$$t(\xi, \eta) = -\frac{1}{\pi} \frac{1}{\sqrt{\eta - \xi}} \int_{-\xi}^{\xi} R(\xi, \eta') \frac{\sqrt{\xi - \eta'}}{\eta - \eta'} d\eta' \tag{3.7}$$

where $\xi = \frac{1}{b\sqrt{2}}(t - bx)$ and $\eta = \frac{1}{b\sqrt{2}}(t + bx)$ for $\xi \leq \eta$. Expressed explicitly in the (x, t) coordinates, Eq. (3.7) is given by

$$r(x, t) = \frac{1}{i\pi} \frac{1}{\sqrt{x}} \int_{bx-t}^0 R(x, t - b(x - x_0)) \frac{\sqrt{x_0}}{x - x_0} dx_0 \tag{3.8}$$

Eq. (3.8) describes the interfacial shear traction due to the remote antiplane loading.

In Section 6, the following two particular loading cases will be discussed. For a shock load $R(x, t) = R_0 H(t)$,

$$t^{\text{shock}}(x, t) = \frac{2R_0}{\pi} \left[\frac{\sqrt{t - bx}}{\sqrt{x}} - \arctan \left(\frac{\sqrt{t - bx}}{\sqrt{x}} \right) \right] H(t - bx) \tag{3.9}$$

For a ramp load $R(x, t) = R_0 t H(t)$,

$$t^{\text{ramp}}(x, t) = \frac{2}{3\pi} R_0 \left[\frac{\sqrt{t - bx}}{\sqrt{x}} (b^2 x + (3 - b)t) - 3t \arctan \left(\frac{\sqrt{t - bx}}{\sqrt{x}} \right) \right] H(t - bx) \tag{3.10}$$

The 'shock' load would correspond to an antiplane contact where the sliding shear force is suddenly applied at $t = 0$; the 'ramp' load to a sliding contact where the shear force is applied gradually and increases linearly with time. The ramp load also serves as an indication of the transient response of the system to alternating loads, the salient features of which may be reproduced by a series of ramp loads of alternating slope.

4. Interfacial shear traction due to a displacement distribution

This is the second problem we are concerned with. In this case, a certain slip displacement $w(x, t)$ is acting along the contact interface. The governing equation remains Eq. (3.1) setting the following boundary value problem:

$$\begin{aligned} \sigma_{yz}(x, 0, t) &= 0 & x \in \mathbb{R}^- \\ u_z(x, 0, t) &= w(x, t) & x \in \mathbb{R}^+ \end{aligned} \tag{4.1}$$

The problem is amenable to solution in a number of ways. For instance, one could invoke the distributed dislocation technique employed by Freund (1974), Burgers and Freund (1980, 1981) and Freund (1998), amongst many others, to solve the problem of a point load applied on the faces of a mode I crack, and also reported by Aki and Richards (2002) in connection with a uniformly propagating shear crack. Such approaches, however, rely on the assumption that $w(x, t)$ is self-similar, i.e., $w(x, t) \sim w(x/t)$ (Freund, 1974). Alternatively, the slip displacement may be converted (in the sense of distributions) into an equivalent force by virtue of the Burridge-Knopoff theorem (Burridge and Knopoff, 1964), and then the representation theorem may be applied to this force distribution. Here, we shall generalise the solution by obtaining the relevant fundamental solution instead.

The solution strategy we adopt here therefore relies on obtaining a fundamental solution for the interfacial shear stress (i.e., the shear stress produced at the interface by a point-like antiplanar displacement), and then achieving the actual solution to the interfacial stress due to the displacement $w(x, t)$ via convolution between $w(x, t)$ and the fundamental solution. This is justified via the representation theorem, which shows that in linear elasticity the displacement and stress fields are isomorphic (Aki and Richards, 2002).

In so doing, we are invoking the linearity between interfacial slip and interfacial stress. Although it is true that the problem we wish to solve is inherently non-linear due to the presence of a frictional force at the interface, it is the interfacial shear stress due that is affected by this non-linearity via the force balance equation (Eq. (2.1)). To wit, the shear stress at the interface is the result of a non-linear force balance. The associated slip distribution, however, will remain linearly dependent on the net interfacial shear stress because the material's inner behaviour remains linear elastic. Note that any potential inelasticity in the constitutive behaviour of the material is neglected here.

4.1. Fundamental solution

Here we first obtain the *fundamental solution*, i.e., the interfacial shear traction associated with a point displacement acting on the contact interface, and then invoke the convolution theorem to obtain the general interfacial traction. Thus, we first wish to solve

$$\begin{aligned} \sigma_{yz}(x, 0, t) &= 0 & x \in \mathbb{R}^- \\ u_z(x, 0, t) &= \delta(x - x_0) \delta(t - t_0) & x \in \mathbb{R}^+ \end{aligned} \tag{4.2}$$

where $x_0 > 0, t_0 > 0$.

This problem is of interest on its own as it clarifies the nature of the fundamental solution. As was commented by Burgers and Freund (1980), it is not immediately obvious how to solve it employing standard procedures such as the Wiener-Hopf method (Noble, 1958). The reasons for this will be discussed below.

Still, we assume that $w(x, t)$ is sufficiently smooth (in principle, at least C^2 and compactly supported over \mathbb{R}^+), that the problem may be solved via Wiener-Hopf. We therefore first extend by continuity the boundary conditions to

$$\begin{aligned} \sigma_{yz}(x, 0, t) &= p_+(x, t) & x \in \mathbb{R} \\ u_z(x, 0, t) &= u_-(x, t) + \delta(x - x_0) \delta(t - t_0) & x \in \mathbb{R} \end{aligned} \tag{4.3}$$

where $p_+(x, t)$ and $u_-(x, t)$ are, respectively, the resultant traction along $x \in \mathbb{R}^+$ and the resultant displacement along $x \in \mathbb{R}^-$; note that $p_+(x, t)$ is in fact the fundamental solution we seek. Both are unknown, and form part of the solution to the boundary value problem.

We begin by defining the following integral transforms:

$$\begin{aligned} \hat{f}(x, y, s) &= \int_0^\infty f(x, y, t)e^{-st} dt, \\ F(k, y, s) &= \int_{-\infty}^\infty \hat{f}(x, y, s)e^{-skx} dx \end{aligned} \quad (4.4)$$

and apply them over the governing equation $\nabla^2 u_z = b^2 \hat{u}_z$, to get

$$\frac{\partial^2 U_z}{\partial y^2} = s^2 \beta^2 U_z(k, y, s) \quad (4.5)$$

where $\beta^2 = b^2 - k^2$.

Applying them over the boundary conditions, which we have extended to apply over the whole line of abscissae, we finally get the following Hilbert problem:

$$-\frac{P_+(k)}{\mu\beta(k)} = U_-(k) + E(k) \quad (4.6)$$

where

$$\begin{aligned} P_+(k) &= s \int_0^\infty \hat{p}_+(x, s)e^{-skx} dx, & U_-(k) &= s^2 \int_{-\infty}^0 \hat{u}_-(x, s)e^{-skx} dx, \\ E(k) &= s^2 \int_0^\infty \hat{u}_z(x, s)e^{-skx} dx \equiv E(k; s) = s^2 e^{-s(t_0+kx_0)} \end{aligned} \quad (4.7)$$

We then proceed to decompose the equation into sectionally analytic functions. To begin with, the first (product) decomposition concerns $\beta(k)$, and is defined as usual (cf. Freund, 1998):

$$\beta(k) = \beta_+(k)\beta_-(k) \Rightarrow \beta_\pm(k) = \sqrt{b \pm k} \quad (4.8)$$

The problems arise in the second (sum) decomposition, which concerns the $S(k; s) = \beta_-(k)E(k; s)$ term. We note here that $x_0 > 0, s > 0$. Thus, the function $S(k; s)$ is bounded only in the $\text{Re}[k] > 0$ half plane, since in the left half plane the exponential term does not generally vanish. Unfortunately, because the term is not bounded for all $|k| \rightarrow \infty$, Liouville's generalised theorem (see Markushevich, 2005a, p.364) will not be satisfied since this theorem explicitly requires that $|S(k)| \leq M \forall k \in \mathbb{C}, M \in \mathbb{R}$ (Markushevich, 2005a; Knopp, 1996), and the usual Wiener-Hopf strategy reliant on the decomposition of the functions into sectionally analytic functions followed by application of the monodromy theorem (see Markushevich, 2005b) and Liouville's generalised theorem (see Noble, 1958; Markushevich, 2005a) is not applicable, because the latter does not hold.

An alternative approach is necessary. Here, we shall follow the one Georgiadis and Charalambakis, 1994 developed for the point load applied on the faces of a confined mode I crack. This technique is, in reality, an extension of the usual analytic continuation techniques (see for instance (Markushevich, 2005b) III 8), and can be justified because albeit it is true that $S(k; s) = \beta_-(k)E(k; s)$ does not fulfil Liouville's generalised theorem, it still satisfies Picard's little theorem (see Markushevich, 2005b).

Therefore, let us divide both sides of Eq. (4.6) by $2\pi i(k - z)$, and then integrate the equation along the imaginary axis with the point z lying on the $\text{Re}[k] > 0$ plane alone. This renders

$$\begin{aligned} \frac{1}{2\pi i} \int_{-i\infty}^{i\infty} \frac{P_+(k)}{\mu\beta_+(k)(k-z)} dk + \frac{1}{2\pi i} \int_{-i\infty}^{i\infty} \frac{\beta_-(k)s^2 e^{-s(t_0+kx_0)}}{k-z} dk \\ = -\frac{1}{2\pi i} \int_{-i\infty}^{i\infty} \frac{\beta_-(k)U_-(k)}{k-z} dk \end{aligned} \quad (4.9)$$

First, we shall tackle the right hand side. We note that as $|k| \rightarrow \infty, \beta_-(k) \sim k^{1/2}$. In addition, we expect that $u_z(x, 0, t) \sim x^{1/2}$ for $x \rightarrow 0$ (cf. Mura, 1982). Invoking the Tauberian theorem (Wiener, 1932), this means that $U_-(k) \sim k^{-3/2}$. Thus, the first integrand in the RHS decays with k^{-1} as $|k| \rightarrow \infty$. We define the branch cut entailed by $\beta_-(k)$ for $\text{Re}[k] > b$, so that the integrand on the right hand side is meromorphic on the $\text{Re}[k] < 0$ half plane.

We can close the contour of integration along the imaginary axis with a semi circle in the $\text{Re}[k] < 0$ half plane, and then invoke Jordan's lemma (see Brown and Churchill, 2009, p.192), by virtue of which the integral along the circular contour vanishes. Since there are no poles enclosed by this contour (by construction z lies on the $\text{Re}[k] > 0$ half plane), then the closed contour integral vanishes, and so does the integral along the imaginary axis.

We further note that $P_+(k) \sim k^{-1/2}$, because we expect that $p_+(x, t) \sim 1/\sqrt{x}$ in the $x \rightarrow 0^+$ limit (see for instance Mura, 1982), so that the integrand decays with k^{-1} as $|k| \rightarrow \infty$. The first integrand has poles in $k = z$ and $k = -b$. We define the branch cut for $\text{Re}[k] < -b$, so we close the contour of integration with a semi circle along the positive half plane, where we know by Jordan's lemma that the integral along the semicircle vanishes. The only pole being $k = z$, we have that by Cauchy's integral theorem:

$$\frac{1}{2\pi i} \int_{-i\infty}^{i\infty} \frac{P_+(k)}{\mu\beta_+(k)(k-z)} dk = \frac{P_+(z)}{\mu\beta_+(z)} \quad (4.10)$$

Thus, we finally find that

$$\frac{P_+(z)}{\mu\beta_+(z)} = -\frac{1}{2\pi i} \int_{-i\infty}^{i\infty} \frac{\beta_-(k)s^2 e^{-s(t_0+kx_0)}}{k-z} dk \quad (4.11)$$

We are now in a position to evaluate the last remaining integral,

$$\int_{-i\infty}^{i\infty} \frac{\beta_-(k)s^2 e^{-s(t_0+kx_0)}}{k-z} dk, \quad (4.12)$$

We note that the integrand is meromorphic with a simple pole at $k = z$ for $\text{Re}[z] > 0$. As noted, it only decays for $\text{Re}[k] > 0$, so we may only close a contour of integration at infinity in the positive half plane. This carries the added complication of coinciding with the branch cut of the integrand, which we define for $\text{Re}[k] > b, \text{Im}[k] = 0$. We close the contour of integration as represented in Fig. 2. Accordingly,

$$\oint = \int_{\text{Im}[k]} + \int_{\Gamma_{\text{Jordan}}} + \int_{\Gamma_{\text{branch cut}}} = 2\pi i \text{Res}[z = k] \quad (4.13)$$

where $\int_{\text{Im}[k]}$ represents the integral along the imaginary axis, $\Gamma_{\text{Jordan}} = |k|e^{i\theta}, |k| \rightarrow \infty, \theta \in (\pi/2, -\pi, 2)$ is the Jordan contour tending to infinity shown in Fig. 2, and $\Gamma_{\text{branch cut}}$ the contour around the branch cut, i.e., $\Gamma_{\text{branch cut}} = (\infty, +b] \cup [+b, \infty)$. Clearly

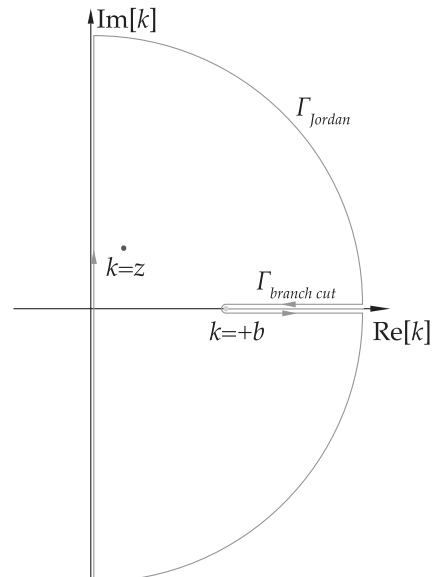


Fig. 2. Contour of integration for Eq. (4.12).

$\int_{\Gamma_{\text{Jordan}}} \rightarrow 0$ by virtue of Jordan's lemma, and $\int_{\text{Im}[k]}$ is the integral of interest here. Thus, the only term in contention is the integral along the branch cut.

The integral along $\Gamma_{\text{branch cut}}$ does not contribute to the residue. Let us define $\Gamma_{\text{branch cut}} = \Gamma_+ + \Gamma_-$ with $\Gamma_- = (\infty, +b]$, $\Gamma_+ = [+b, \infty)$. If we set $k - b = re^{i\theta}$ for $\theta = 0$ along Γ_- and $\theta = 2\pi$ along Γ_+ , so that $\Gamma_- \equiv r \in (\infty, 0]$, $\Gamma_+ \equiv r \in [0, \infty)$, we find that

$$\int_{\Gamma_{\pm}} \frac{\sqrt{r}e^{i\theta/2}}{b + re^{i\theta} - z} dr \Rightarrow \int_{\Gamma_-} = - \int_{\Gamma_+} \quad (4.14)$$

upon changing $\theta = 0$ for $\theta = 2\pi$.

Thus, we have that:

$$\frac{P_+(z)}{\mu\beta_+(z)} = -s^2 e^{-st_0} \beta_-(z) e^{-szx_0} \quad (4.15)$$

4.1.1. Inversion of the $\beta(z)e^{-szx_0}$ term. This is the sole non-vanishing term contributing to the fundamental solution. Its inversion can be readily achieved through the Cagniard-de Hoop method (De Hoop., 1960; Cagniard, 1939), as we detail here. We first write the inversion in k^2 :

$$\hat{p}_+(x, s) = -s^2 e^{-st_0} \mu \frac{1}{2\pi i} \int_{-i\infty}^{i\infty} \beta(z) e^{-szx_0} e^{szx} dz \quad (4.16)$$

We set $\tau = -z(x - x_0) \equiv -z\tilde{x}$, and distort the integration path by closing it along the $\text{Re}[z] > 0$ half plane for the case when $\tilde{x} > 0$ and along $\text{Re}[z] < 0$ for the case when $\tilde{x} < 0$, in a manner analogous to what was done in Fig. 2 when evaluating Eq. (4.12). We now have two branch cuts, defined for $k \in (-\infty, -b] \cup [b, \infty)$. Avoiding either results in a contribution, again analogous to the one obtained when evaluating Eq. (4.12), which invoking Schwartz's reflection principle leads to

$$\hat{p}_+(x, s) = \frac{s^2 e^{-st_0} \mu}{\pi \tilde{x}} \int_0^{\infty} \text{Im} \left[\beta \left(-\frac{\tau}{\tilde{x}} \right) \right] H(\tau - b\tilde{x}) d\tau \quad (4.17)$$

Upon inverting in time, and invoking the properties of the Laplace transform, we finally obtain:

$$p_+(x - x_0, t - t_0) = \frac{b^2 \mu H(t - t_0 - b|x - x_0|)}{\pi \left((t - t_0)^2 - b^2(x - x_0)^2 \right)^{3/2}} \quad (4.18)$$

which is the fundamental solution we were seeking.

4.2. Interfacial shear traction through convolution and distributed dislocations

The interfacial shear traction $s(x, t)$ due to the unknown slip displacement distribution $w(x, t)$ may then be obtained through convolution with the fundamental solution Eq. (4.18):

$$s(x, t) = \int_{\mathbb{R}} \int_0^t w(x_0, t_0) \frac{b^2 \mu}{\pi \left((t - t_0)^2 - b^2(x - x_0)^2 \right)^{3/2}} H(t - t_0 - b|x - x_0|) dx_0 dt_0 \quad (4.19)$$

We note that $s(x, t) = fN(x, t) - r(x, t)$ is known, so in principle Eq. (4.24) expresses an integral equation with $w(x, t)$ as its unknown. The equation does not appear to have a direct analytical solution, so besides asymptotic approaches, a numerical scheme is the only tool left available to explore the transient contact problem. However, we note that the kernel $p_+(x, t)$ of Eq. (4.24) is of order -3 with a dimensionality of 2, which makes the integral hypersingular (cf. Vainikko, 1993; Muskhelishvili, 1953) and fundamentally ill-posed (cf. Renardy, 1992). This prevents an easy numerical solution, to which Section 6 is devoted.

The solution to this passes through the distributional properties of the convolution. In the sequel, and for simplicity we take the relative slip displacement $w(x, t)$ to be defined about the edge of the contact region (i.e., $w(0, t) = 0$). We note (cf. Aki and Richards, 2002) that we may express $w(x, t)$ as:

$$w(x, t) = \frac{\partial w(x, t)}{\partial t} \int_{[0, t] \times [0, x]} dw(x' \times t') = \int_0^x \int_0^t \frac{\partial^2 w(x', t')}{\partial x' \partial t'} dx' dt' = \int_0^{\infty} \int_0^{\infty} \frac{\partial^2 w(x', t')}{\partial x' \partial t'} H(t' - t) H(x' - x) dx' dt' \quad (4.20)$$

where we have exploited the fact that by construction the support of $w(x, t)$ is $t > 0, x > 0$. We may express this as

$$w \equiv \langle w''_{xt}, H(t)H(x) \rangle \quad (4.21)$$

where $\langle f, g \rangle = f * g$ is the convolution, $w''_{xt} = \partial_x \partial_t w$ in Lagrange notation, and where $H(t)H(x) \equiv u_{\text{dis}}(x, t)$ represents the interfacial slip due to an unitary injected screw dislocation (cf. Markenscoff, 1980; Verschueren et al., 2017; Gurrutxaga-Lerma, 2017). Now, since $s(x, t)$ is given by

$$s = \langle w, p_+ \rangle = \langle \langle w''_{xt}, u_{\text{dis}} \rangle, p_+ \rangle = \langle w''_{xt}, \langle u_{\text{dis}}, p_+ \rangle \rangle \quad (4.22)$$

The term $\tau(x, t) \equiv \langle u_{\text{dis}}, p_+ \rangle$ represents, of course, the interfacial shear traction due to a screw dislocation acting along the contact interface. Therefore, Eq. (4.22) generalises Freund's Freund (1974) and Aki and Richards (2002) approaches of expressing the displacement function as the sum of contributions due to dislocations of infinitesimal magnitude, themselves derived from Leibfried (1951) original static distributed dislocation technique. The use of distributed dislocation solutions in static contact and static fracture mechanics problems is well established Hills et al. (1996); the model we employ here arises as the natural elastodynamic extension to these.

In the following, we shall call $w''_{xt} = b(x, t)$ for simplicity, and focus on it, since w may be recovered from b using Eq. (4.20). Here $b(x, t)$ represents loosely speaking the spatio-temporal gradient of a (normalised) Burgers vector distribution, but it lacks any crystallographical significance that would relate it to the theory of dislocations: the dislocations under consideration here are not crystallographic dislocations, but a mathematical device to model kernels of strain.

We must first find the interfacial shear traction $\tau \equiv \langle u_{\text{dis}}, p_+ \rangle$ due to a screw dislocation acting along the contact interface, which is immediately accessible via convolution with $p_+(x, t)$, rendering

$$\tau(x, t) = \frac{\mu}{\pi} \frac{\sqrt{t^2 - b^2 x^2}}{tx} H(t - bx) \quad (4.23)$$

This entails that

$$s(x, t) = \frac{\mu}{\pi} \int_0^t \int_0^{x-1/b(t-t_0)} b(x_0, t_0) \frac{\sqrt{(t - t_0)^2 - b^2(x - x_0)^2}}{(t - t_0)(x - x_0)} dx_0 dt_0 \quad (4.24)$$

is the alternative form of the interfacial shear traction due to the displacement distribution $w(x, t)$, in this case weakly singular. This form can only be given under the assumption that $w(x, t)$ is at least C^2 - i.e., that $b(x, t)$ exists and is generally compactly supported over the positive axis of abscissae.

5. The normal contact load

A remote normal load is required to ensure the contact between the two elastic half spaces. Here, we regard this normal load independent from the remote antiplane shear load (Barber, 2018) and, as a result, in the absence of frictional forces the normal load plays no part in the shear contact problem (Barber, 2018; Johnson, 1987).

² Note that the scaling factor s carried over by the differential measure cancels with the $1/s$ factor pre-multiplying $P_+(z)$ when performing inversion.

However, given that here we wish to consider the presence of friction as well as slip, we need to offer an account of the normal interfacial load. The resulting problem shall then mirror the usual elastostatic problems.

In the most general and protracted case, the contact is established and maintained by a certain remote normal load, which in the sequence we express with the function $P(x, t)$. The function $P(x, t)$ must be such that it ensures that the two half surfaces remain in contact, but no further desideratum is imposed a priori. We wish to find a general formula for the interfacial normal force $N(x, t)$ arising as a result of the application of $P(x, t)$, since $N(x, t)$ induces the frictional force.

That is, the resulting problem is an in-plane problem where a remote load $P(x, t)$ induces an interfacial ‘contact’ pressure over a half line. This is a classical problem in dynamic fracture (Freund, 1998), corresponding to the remote loading of a quiescent (i.e., non-propagating) mode I crack, a partial solution to which may be found in Miklowitz (1978) and Freund (1998) for the case of suddenly applied, constant remote loads. Although the normal contact load is described as corresponding to a mode I crack’s normal stress along the epicentral line, the problem under consideration here is not a fracture problem: the interface exists by virtue of the remote normal load, and we merely wish to model its interfacial normal stress, which happens to be given by a mode I crack’s stress field (see Hills et al., 1996; Dini et al., 2005; Dini et al., 2004).

The resulting expressions for the interfacial normal traction cannot generally be given in explicit form. This is because they depend on the inverse of the Rayleigh function. For instance, for a shock load of magnitude N_0 these are (see Freund, 1998, Ch.2):

$$N_+(x, t) = -\frac{1}{\pi x} \int_{ax}^t \text{Im}[\Sigma_+(-\tau/x)] d\tau, \quad \Sigma_+(k) = \frac{N_0}{k} \left(\frac{F_+(0)}{F_+(k)} - 1 \right) \tag{5.1}$$

and

$$F_+(k) = \frac{\sqrt{a+k}}{(c_R+k)S_+(k)},$$

$$\ln S_+(k) = -\frac{1}{\pi} \int_a^b \frac{1}{\tau+k} \arctan \left[\frac{4\tau^2 \sqrt{(\tau^2-a^2)(b^2-\tau^2)}}{(b^2-2\tau^2)^2} \right] d\tau \tag{5.2}$$

where $a = 1/c_l$ is the longitudinal slowness of sound (and c_l the longitudinal speed of sound), and c_R the Rayleigh wave speed.

However, as is done in the elastostatic case (Barber, 2018), the interfacial normal traction field about the edge of the contact zone can be asymptotically treated as a near field Williams expansion. In the elastodynamic case, we have that (Freund, 1998),

$$N(x, t) \approx \frac{K_I(t)}{\sqrt{2\pi x}} \tag{5.3}$$

where $K_I(t)$ is the dynamic stress intensity factor, and depends on the nature of the dynamic remote load. For a suddenly applied shock load (Freund, 1998) of magnitude N_0 ,

$$K_I^{\text{shock}}(t) = 2N_0 \frac{\sqrt{(1-2\nu)t}}{(1-\nu)\sqrt{a\pi}} \tag{5.4}$$

In a more general loading case, $K_I(t)$ will be dependent on the load history. If the remote $P(x, t)$ load is such that its time history can be separated from its spatial variation (i.e., $P(x, t) = P(x)h(t)$), then (Ravi-Chandar, 2004; Freund, 1998)

$$K_I(t) = \int_0^t K_I^{\text{shock}}(\tau) \frac{\partial h(\tau)}{\partial \tau} d\tau \tag{5.5}$$

For instance, for a ramp:

$$K_I^{\text{ramp}}(t) = 4N_0 \frac{t\sqrt{(1-2\nu)t}}{3(1-\nu)\sqrt{a\pi}} \tag{5.6}$$

In the following, we shall employ the asymptotic near fields of the mode I crack to given by Eq. (5.3) as a reasonable model for the normal traction about the edge of contact zone. Unless otherwise stated, we shall focus on the shock loaded normal load, which serves to model the sudden change of the applied remote normal load.

6. The force balance equation

In view of Eqs. (3.8) and (4.24), the force balance at the interface becomes the following integral equation:

$$\frac{\mu}{\pi} \int_0^t \int_{\Gamma} b(x_0, t_0) \frac{\sqrt{(t-t_0)^2 - b^2(x-x_0)^2}}{(t-t_0)(x-x_0)} dx_0 dt_0$$

$$= fN(x, t) - \frac{1}{i\pi} \frac{1}{\sqrt{x}} \int_{bx-t}^0 R(x, t - b(x-x_0)) \frac{\sqrt{x_0}}{x-x_0} dx_0 \tag{6.1}$$

where as in Eq. (4.24), $\Gamma \equiv [0, x + 1/b(t_0 - t)]$. We rewrite Eq. (6.1) as

$$\langle \tau(x, t), b(x, t) \rangle = F(x, t) \tag{6.2}$$

where

$$F(x, t) = fN(x, t) - \frac{1}{i\pi} \frac{1}{\sqrt{x}} \int_{bx-t}^0 R(x, t - b(x-x_0)) \frac{\sqrt{x_0}}{x-x_0} dx_0 \tag{6.3}$$

for a general loading $N(x, t)$ and $R(x, t)$. We note that $F(x, t)$ has compact support for $t > 0, x > 0$ and $bx < t$, and that $\tau(x, t)$ is to all effects a convolution kernel (cf. Porter and Stirling, 1990). In addition, the kinematic condition that $\text{sign}(\partial_t u_z) = -\text{sign}(q(x, t))$ must be satisfied. It is worth pointing out that Eq. (6.2) is of a similar nature to the dynamic Peierls-Nabarro equation discussed by Pellegrini (2010, 2014) in the context of mobility laws for straight dislocations, although not generally self-similar. As such, general solutions will be unachievable but numerically; particular ones for simple loadings may still be found as we describe below.

6.1. Static loading and static limit

Eq. (6.2) captures only the transient contribution to the general contact problem. This may be appreciated in the form of its solution: because the slip convolution integral Eq. (6.1) offers compact support over $t - bx > 0$, then $b(x, t)$ (and $w(x, t)$) must be compactly supported over the said interval. This means that the region of slip due to the transient solution to Eq. (6.2) will at most be an ever expanding region within the cone $t - bx > 0$, and will not support any loading applied away from it. This has been imposed by construction upon assuming that the loading begins at $t > 0$. This means that mixed-type problems where, say, the contact pressure is time-independent quasistatic but the remote shearing force is time dependent must be solved via superposition of the static solution under a frictional force and no remote shearing load (see Barber, 2018 for further details), and the transient solution given by Eq. (6.2) for frictionless case.

We also note that in the static limit Eq. (6.2) becomes the standard static antiplane contact equation. The static limit may be found requiring $t \rightarrow \infty$ or, alternatively, $\rho \rightarrow 0$ (and $b \rightarrow 0$), since in the latter limit perturbations travel instantaneously:

$$\lim_{t \rightarrow \infty} \tau(x, t) = \lim_{t \rightarrow \infty} \frac{\sqrt{t^2 - b^2 x^2}}{tx} = \frac{1}{x} \tag{6.4}$$

so the convolution becomes

$$\lim_{t \rightarrow \infty} \langle \tau(x, t), b(x, t) \rangle = \frac{\mu}{\pi} \int_0^a \frac{\dot{b}(x_0)}{x - x_0} dx_0 = \frac{\mu}{\pi} \int_0^a \frac{w(x_0)}{(x - x_0)^2} dx_0 \quad (6.5)$$

for a slip region over $x \in [0, a]$, and where $\dot{b}(x)$ represents the slip velocity. This integral is analogous to the one employed in describing the interfacial shear load σ_{xz} due to a distributed dislocation (cf. Barber, 2018).

6.2. Numerical solution of the contact problem

Owing to the weakly singular nature of the integral kernel, we may produce a relatively simple general numerical scheme for the solution of Eq. (6.2) based on the collocation-Nyström method (Porter and Stirling, 1990; Vainikko, 1993). The solution to multidimensional integral equations using such schemes is commonplace in the literature, and a detailed description of these methods might be found in Atkinson (1997) and Vainikko (1993). Application of such methods in the context of elastic defects can be found in Martin and Rizzo (1989) for static cracks, and Nishimura and Kobayashi (1989) for elastodynamic cracks in anisotropic bodies, amongst many others.

Here, we largely follow the method laid out in Nishimura and Kobayashi (1989) and Martin and Rizzo (1989). Let $S(t) = [0, x_{\max}] \times [0, t_{\max}] \subset \mathbb{R}^+ \times \mathbb{R}^+$ be the computation space. Because the problem is one of propagating waves, $x_{\max} \in \mathbb{R}^+$ can be arbitrarily large for finite times, but for numerical purposes, we must ensure that the maximum allowable abscissa x_{\max} is not reached before the maximum allowable time t_{\max} , so we require $x_{\max} < t_{\max}/b$.

We define some *a priori* arbitrary partition $\{x_i\}_{i=0}^{n_x}, \{t_j\}_{j=0}^{n_t}$ of $S(t)$. This allows us to specify the intervals $S_{ij} = [x_i, x_{i+1}] \times [t_j, t_{j+1}]$ over which we shall discretise the solution, where $(x_0, t_0) = (0, 0)$ and $(x_{n_x}, t_{n_t}) = (x_{\max}, t_{\max})$.

We define a basis function set $\{N_{ij}(x, t)\}$ offering compact support over $[x_i, x_{i+1}] \times [t_j, t_{j+1}]$. We do so in order to be able to express the Burgers vector gradient $b(x, t)$ as

$$b(x, t) = \sum_{i=0}^{n_x} \sum_{j=0}^{n_t} b_{ij} N_{ij}(x, t) \quad (6.6)$$

with $b_{ij} \in \mathbb{R}$ is a number.

Inserting Eq. (6.6) into Eq. (6.2), we obtain

$$\begin{aligned} F(x, t) &= \sum_{ij} b_{ij} \int_0^t \int_{\Gamma} N_{ij}(x_0, t_0) \tau(x - x_0, t - t_0) dt_0 dx_0 \\ &= \sum_{ij} b_{ij} K_{ij}(x, t) \end{aligned} \quad (6.7)$$

where $\sum_{ij} \equiv \sum_{i=0}^{n_x-1} \sum_{j=0}^{n_t-1}$, and

$$K_{ij}(x, t) = \int_0^t \int_{\Gamma} N_{ij}(x_0, t_0) \tau(x - x_0, t - t_0) dt_0 dx_0 \quad (6.8)$$

which is well-defined for each set of basis functions.

Typically, in Nyström-like methods Eq. (6.8) would be solved via numerical quadrature (see Atkinson, 1997). However, as observed by Martin and Rizzo (1989), if we prescribe the basis functions $N_{ij}(x, t)$ to be simple enough $C^{1 \times 1}$ functions, the analytic form of $K_{ij}(x, t)$ may in this case be derived a priori. Thus, let $x_{i+1} - x_i = \Delta x_i$ and $t_{j+1} - t_j = \Delta t_j$ be the width of the $i \times j$ interval. We may then use a basis set formed by pulse functions in time, and piecewise linear *shape functions* in space, i.e., with $N_{ij}(x, t)$ on

$[x_i, x_{i+1}] \times [t_j, t_{j+1}]$ of the form:

$$N_{ij}^{\text{linear pulse}}(x, t) = \begin{cases} \frac{x - x_i}{\Delta x_{i-1}} & (x, t) \in [x_{i-1}, x_i] \times [t_j, t_{j+1}] \\ \frac{x_{i+1} - x}{\Delta x_i} & (x, t) \in [x_i, x_{i+1}] \times [t_j, t_{j+1}] \\ 0 & \text{otherwise} \end{cases} \quad (6.9)$$

These basis functions are equivalent to the constant velocity over fixed time intervals discretisation employed by Pellegrini (2014) in studying the mobility law of a dislocation.

Upon integration of Eq. (6.8) renders (for $t_j < t, x_i < x$)

$$\begin{aligned} K_{ij}^{\text{linear pulse}}(x, t) &= \begin{cases} \frac{1}{\Delta x_{i-1}} L_{ij}(x - x_i, t - t_j) \\ -\frac{1}{\Delta x_i} L_{ij}(x - x_i, t - t_{j+1}) & (x, t) \in [x_{i-1}, x_i] \times [t_j, t_{j+1}] \\ \frac{1}{\Delta x_{i-1}} L_{ij}(x - x_{i+1}, t - t_j) \\ -\frac{1}{\Delta x_i} L_{ij}(x - x_{i+1}, t - t_{j+1}) & (x, t) \in [x_i, x_{i+1}] \times [t_j, t_{j+1}] \end{cases} \end{aligned} \quad (6.10)$$

where

$$L_{ij}(x, t) = \frac{1}{\pi} \left[\frac{\sqrt{t^2 - b^2 x^2}}{bx} + i \ln \left(\frac{bx + i\sqrt{t^2 - b^2 x^2}}{t} \right) \right] H(t - bx) \quad (6.11)$$

is obtained from integrating $\langle K, N_{ij} \rangle$. On more refined computations, one may employ higher order basis sets in time and space as required (see for instance (Vainikko, 1993), Ch.7, and Atkinson (1997), Ch. 5).

A final provision is necessary for the initial interval owing to the fact that it is subjected to a $1/\sqrt{x}$ singularity on the external load $F(x, t)$. Here we adopt the commonly employed technique (Henshell and Shaw, 1975; Barsoum, 1976) of making the initial interval $[0, x_1]$ a fourth of the regular size. Thus, for $[0, x_1]$ we set $\Delta x_0 = 1/4 \Delta x$, with the shape function being

$$N_{0j}(x, t) = \frac{x_1 - x}{\frac{1}{4} \Delta x} H(x) H(t) \quad (x, t) \in [x_0, x_1] \times [t_j, t_{j+1}] \quad (6.12)$$

The resulting problem consists of $n_x \times n_t$ unknowns (the b_{ij} coefficients). As done by Nishimura and Kobayashi (1989) in order to find them we shall *collocate* as many points: we choose to evaluate $F(x, t)$ and $K_{ij}(x, t)$ at a discrete set of (x, t) *collocation points* located within each $[x_i, x_{i+1}] \times [t_j, t_{j+1}]$ interval. Collocating within the integration interval has the advantage of almost diagonalising the problem due to the compact support provided by the basis functions in the $i \times j$ interval (cf. Nishimura and Kobayashi, 1989). For simplicity, and aside from the initial interval, we choose intervals of constant length in space and time, i.e., $\Delta x_i \equiv \Delta x = \text{constant}$ and $\delta t_j \equiv \Delta t = \text{constant}$, so that all the collocation points may be given as $(x, t) = (x_k, t_l) = (x_k + k, t_l + l)$ for (x_k, t_l) nodes of the interval discretisation, and $k \leq \Delta x, l \leq \Delta t$. We empirically find that $k = 0.5 \Delta x$ and $l = 0.9 \Delta t$ appear to produce the most stable results. Thus, we are effectively bound to solve the following problem:

$$F_{kl} = \sum_{i=0}^{n_x} \sum_{j=0}^{l-1} b_{ij} K_{ijkl} \quad (6.13)$$

where we use $F_{kl} \equiv F(x_k + k, t_l + l)$, $K_{ijkl} \equiv K_{ij}(x_k - x_i + k, t_l - t_j + l)$. This is a simplified deconvolution problem, owing to the fact that the summation in j finishes for $j < l$.

The problem can be easily solved by iterating through the time variable. For $l = 0$, $F_{k0} = 0$ trivially. For $l = 1$,

$$F_{k1} = \sum_{i=0}^{n_x} b_{i0} K_{i0k1} \quad (6.14)$$

is a standard matricial problem from which b_{i0} might be found. For $l = 2$,

$$F_{k2} = \sum_{i=0}^{n_x} (b_{i0} K_{i0k2} + b_{i1} K_{i1k2}) \quad (6.15)$$

where we use b_{i0} to compute b_{i1} . Subsequent time steps depend on the solution to previous ones.

The kinematic consideration that $\text{sign}(\partial_t w) = -\text{sign}(q(x, t))$ is checked for each step l in the solution. This is done by computing through numerical integration the spatial integral of $b(x, t)$, $\partial_t w = \int_x b(x, t) dx$, which can be readily achieved through spatial integration of the basis functions,

$$\partial_t u_z(x, t) = \int_0^x b_{ij} N_{ij}(x', t) dx' \quad (6.16)$$

If the sign of $\partial_t u_z(x, t)$ is found to be incorrect over some spatial interval \bar{x}_{sign} , the sign in front of the frictional force in Eq. (6.2) is reversed over that interval, and the b_{ij} solution for time step l is recalculated. The same sign check is performed anew, and if necessary the sign of the frictional force is again reversed, until sign convergence is achieved. In general, we have observed that over two or three re-iterations of the same time step convergence is achieved, and the sign reversal is carried through to the following steps. Further comments on the need for and implications of this kinematic contact condition are discussed below in Section 6.4.

The displacement field may be obtained from integrating Eq. (6.6), which leads to

$$w(x, t) = \sum_{i,j} b_{ij} M_{ij}(x, t) \quad (6.17)$$

where

$$M_{ij}(x, t) = \left[(t - t_j)H(t - t_j) + (t_{j+1} - t)H(t - t_{j+1}) \right] \left(\frac{1}{2}(x - x_i)^2 H(x - x_i) - \frac{1}{2}(x - x_{i+1})^2 H(x - x_{i+1}) \right) \quad (6.18)$$

with the requirement that $w(0, 0) = 0$.

The method here described provides a sufficiently stable algorithm for frictionless loading. However, if the frictional loading arises from a sudden load, the ensuing problem is essentially ill-posed (cf. Renardy, 1992; Martins et al., 1995) and the algorithm has to be modified to ensure it remains stable. As is commonly done in deconvolution problems, here we chose to mollify the solution over each time step using a Tikhonov filter (Hansen et al., 2006; Tikhonov and Arsenin, 1977) (that is, a Tikhonov regularisation using a singular value decomposition). Thus, for each time step we compute a filtered solution $b_{\text{filt}}(x, t)$ of the form

$$b_{il}^{\text{filt}} = \sum_k^{n_t} \phi_k b_{il} \quad (6.19)$$

where

$$\phi_k = \frac{\sigma_k}{\sigma_k^2 + \alpha} \quad (6.20)$$

is the filter factor, and σ_k the singular values of b_{ij} , and α the Tikhonov regularisation parameter. The Tikhonov regularisation parameter was computed using Morozov's discrepancy principle (see Hansen et al. (2006)). The filtered solution is used to propagate the solution over to the next time step, which is filtered in turn. The filter has an effect of stabilising the solution, and of mollifying sudden changes (i.e., steps).

6.3. Frictionless contact

Consider a loading regime where the normal load is static (i.e., contact is enforced by a time-independent normal load, notionally since $t \rightarrow -\infty$). Say that at time $t = 0$ the shearing load starts to change in value, and therefore becomes time dependent. For example, assume that for $t > 0$ the remote shearing load may acquire time independent and time dependent components, say $R(x, t) = R_{\text{static}} + R_{\text{dynamic}}(x, t)$. Because the normal load remains static, the frictional forces imposed by Amonton's law are time-independent and static as well, and the ensuing frictional contact problem, which may include the R_{static} time independent component of the shearing load if there is any, may be studied using the usual elastostatic solutions (see Barber, 2018; Hills and Nowell, 1994; Johnson, 1987 for such solutions).

However, the shearing contact problem becomes dynamic under the influence of $R_{\text{dynamic}}(x, t)$, and must be studied as an elastodynamic, frictionless contact, i.e., obeying Eq. (6.2) with $f = 0$. The complete problem (static frictional and frictionless dynamic) may be obtained by superposing the solutions to each of the sub-problems. Thus, the elastodynamic frictionless problem may be understood as the time dependent deviation from the static solution. Here we study the significance of the solution to the latter; by construction, contact is guaranteed to exist by the normal load, and in the absence of friction the elastodynamic solution will first and foremost offer a measure of the changes in the relative displacement between the two surfaces. That is, the frictionless problem under consideration here seeks to answer: given an interfacial shear load $r(x, t)$, how much would the interface have to slip to ensure that the net interfacial shear load is zero?

Solving Eq. (6.2) with $f = 0$ numerically as we described in Section 6.2, we achieve the solutions depicted in Figs. 3 and 4. These two figures compare at different instants in time the magnitudes of $b(x, t)$ and $w(x, t)$ for a shock load and a ramp load shearing load, respectively. As can be seen, the solution for $b(x, t)$ vanishes for $x > bt$, and is non-zero and divergent at the origin; this is in response to the equally divergent loads. The slip displacement $w(x, t)$ grows in magnitude from the origin to reach a time-varying but constant value in what may be deemed the transient stick region; in this, the transient response resembles the elastostatic response of the classic Cattaneo-Midlin problem (cf. Barber, 2018).

The magnitude of $b(x, t)$ is of opposite sign to the shearing load's, indicating the need to distribute negative screw dislocations to accommodate a positive shearing load. The ensuing slip $w(x, t)$ is also negative; this is consistent with the expectation in the elastostatic Cattaneo-Midlin problem a relative increase in the shearing load results in a relative increase in the slip area (Barber, 2018). Initially, the shock load produces the strongest variation in both $b(x, t)$ and $w(x, t)$, but we do not observe a significant change in the qualitative behaviour of the solution when we impose a ramp load instead: in both cases the transient load propagates as a wave, and the area of transient slip is bounded by the transverse speed of sound itself, for $x < c_t t$. All points not reached by the propagating loads (i.e., all $x > c_t t$) are points of transient stick. This transient stick is inherently different to the elastostatic stick: it exists solely because causality requires that at some $t > 0$ not all points of the contact interface be loaded. In Figs. 3 and 4 the transient stick is demarcated by a plateau in the value of $w(x, t)$, and a zero value in the Burgers vector density gradient $b(x, t)$, consistent with the expectation that no distributed dislocations are necessary to accommodate stick.

The transient slip is also inherently different to the elastostatic slip. For one thing, Fig. 4 would suggest that if sufficient time is allowed for the slip region to develop, the whole interface would slip. Albeit this is true for the ramp load solution, it is not true for the shock loading one. This is because whereas the magnitude

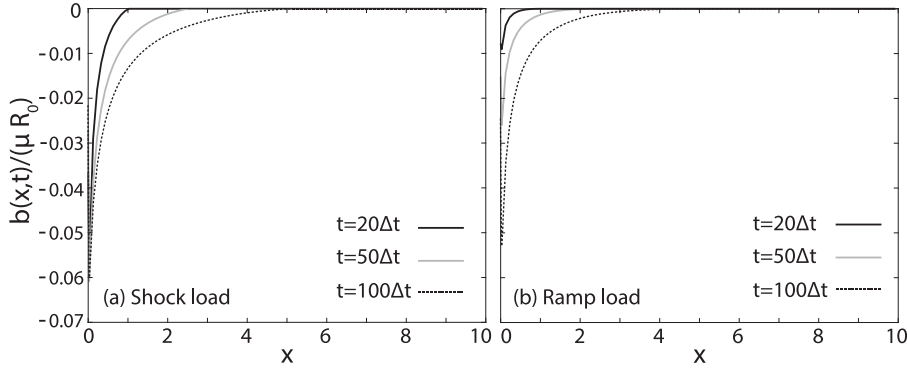


Fig. 3. Burgers vector gradients at different time steps for (a) a frictionless shock shearing load (Eq. (3.9)) and (b) a frictionless ramp shearing load (Eq. (3.10)). Here $R_0 = 1$, $b = 1/10$, $\Delta x = 0.1$, $\Delta t = 0.005$ with a mesh size of $n_x = 100$, $n_t = 100$.

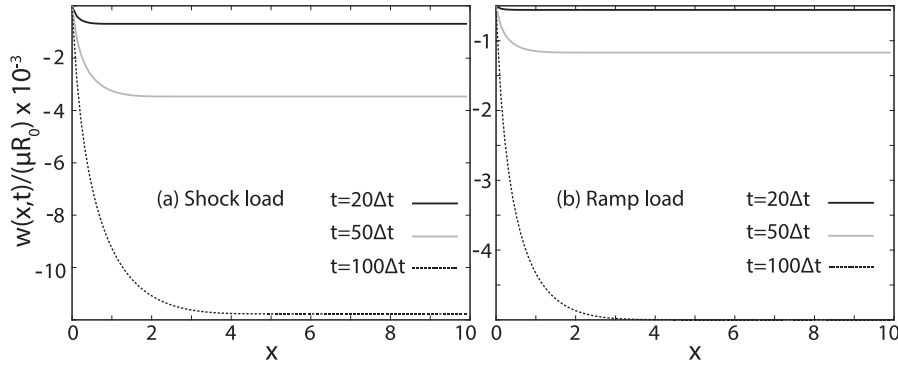


Fig. 4. Slip displacement at different time steps for (a) a frictionless shock shearing load (Eq. (3.9)) and (b) a frictionless ramp shearing load (Eq. (3.10)). Here $R_0 = 1$, $b = 1/10$, $\Delta x = 0.1$, $\Delta t = 0.005$ with a mesh size of $n_x = 100$, $n_t = 100$.

of the ramp load monotonically increases over time and, therefore, there is an increasing need to accommodate an ever increasing interfacial shear traction (which increases with $t^{3/2}$), the shock load solution (Fig. 3) saturates over time to the elastostatic prediction. This may be appreciated in Fig. 3a, where for the shock load the magnitude of the Burgers vector density does not increase over time at the edge of the contact interface, whereas in Fig. 4a the magnitude of the Burgers vector density at the edge of the contact area increases in time. This increase in magnitude propagates inwards, so that over time the slip distribution of a ramp load will come to occupy the whole interface. The shock load tends to saturate to the elastostatic interfacial shear traction, and as such will come to be governed by the same contact considerations that control the Cattaneo–Midlin problem.

6.4. Frictional contact

Friction plays an important role in the nature of the dynamic contact. In the numerical solutions we present in the following, we set $F_{\text{fric}}(x, t) < 0$ and $s(x, t) > 0$ (see for instance Hills and Nowell, 1994, p.12), so that the signs depicted in Eq. (6.1) are a priori correct. We expect that the shearing tractions act in opposite direction to the sliding between the two surfaces, under the assumption that $w(x, t) > 0$. As will be discussed below, these considerations are to be corrected in the dynamic case to account for the kinematic contact condition and the time varying nature of the contact loads. As in the frictionless case, we explore the cases of shock and ramp shear loads. In this case however, we allow the magnitude of the remote normal and shear loads to vary independently from one another. In order to parametrise better the effect these two loads have on one another, we introduce the parameter $\xi = R_0/(fN_0)$, so that a small ξ entails a large frictional force, and a large ξ a weak one, relative to the magnitude of the

remote shearing load. Unless otherwise stated, the same numerical parameters as those employed in the frictionless case were used: $R_0 = 1$, $b = 1/10$, $\Delta x = 0.1$, $\Delta t = 0.005$ with a mesh size of $n_x = 100$, $n_t = 100$, and fN_0 determined from the choice of ξ .

Figs. 5 and 6 depict the magnitudes of $b(x, t)$ and $w(x, t)$ for different ξ under shock loading. As in the frictionless case, the solution always has a region of transient ‘stick’, which is defined relative to the edge of the contact zone by the region unreached by the loading wave at some instant in time. In that sense, the transient ‘stick’ is inherently different to the elastostatic stick, given that in the former the condition that $|q(x, t)| \leq fN(x, t)$ is trivially fulfilled for all $x > t c_t$, simply because the loading, travelling at the transverse speed of sound, lacks sufficient time to reach the current region of stick.

The slip zones we describe here apply best for the instants in time following the onset of the loading. Thus, we do not observe a steady state stick-slip zone of the sort that would be found in the elastostatic Cattaneo–Midlin problem. In fact, with our underlying assumptions we cannot reach the steady state. This is because in Section 5 we have modelled the frictional load using the asymptotic normal elastodynamic field of a quiescent mode I crack. These asymptotic fields are monotonically increasing with $t^{1/2}$ (see Eq. (5.5)), which means that unless a reflected ‘release’ wave were to reach the interface, the near field of a mode I crack is unbounded in time as well as space. In order to reach a stationary solution at $t \rightarrow \infty$, we would be required to employ the full solution (see Freund, 1998). The quality of the asymptotic fields we employ here is nonetheless good over relatively short periods of time (Ravi-Chandar, 2004; Freund, 1998), and indeed the far field of the full solution increases with $t^{3/2}$ (Gurrutxaga-Lerma, 2018), which suggests the near field dominates the response for $t < bL$, L some characteristic length-scale of the problem. Over longer periods of time, the steady state ‘static’ solutions can only be reached

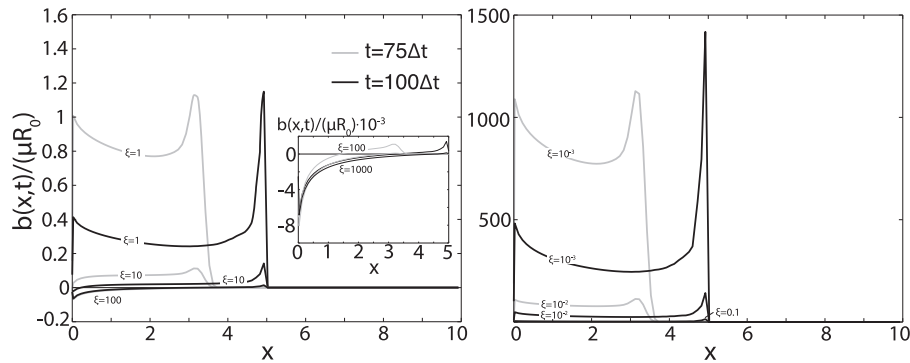


Fig. 5. Magnitude of $b(x, t)$ for different $\xi = R_0/(fN_0)$ ratios under shock loading. The value of $b(x, t)$ for very large ξ are represented in the inset. The same numerical solution parameters as those employed in the frictionless case were used.

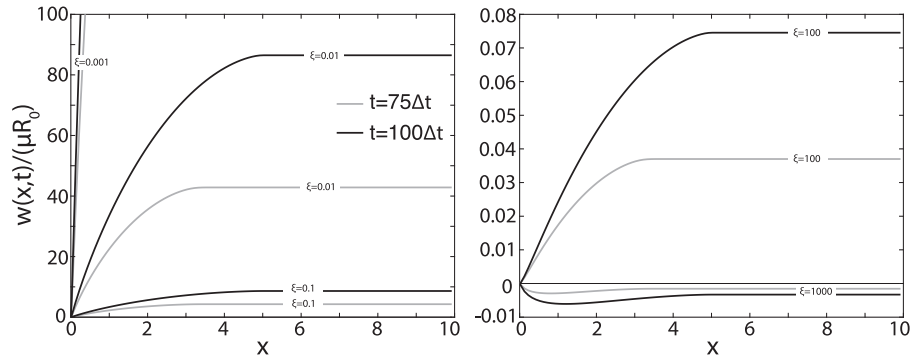


Fig. 6. Magnitude of $w(x, t)$ for different $\xi = R_0/(fN_0)$ ratios under shock loading. Those values of ξ more representative of characteristic features of the solution are represented. The same numerical solution parameters as those employed in the frictionless case were used.

if there are free surfaces involved; this would entail considering a finite sized problem that would undoubtedly modify the solutions considered here. Thus, the solution we are modelling here is relevant for short periods of time, and therefore best suited to study the transient response.

In the wake of the transient stick region, there arises a region of slip. It is in this slip region that we observe strong qualitative and quantitative differences between the frictionless and frictional loading cases. In particular, as may be seen in Fig. 5, for large values of ξ the shock load is found to lead to regions where $w(x, t) < 0$, i.e., of the same sign as the frictional force. Such regime of *reverse slip* is triggered because for large enough ξ , the frictional force is very weak compared to the shearing force, which comes to dominate the contact response as in the frictionless case. For larger values of the frictional force relative to the shearing force (i.e., low ξ), the frictional force comes to dominate the slip distribution gradients $b(x, t)$, which becomes positive (see Fig. 5); the slip distribution also becomes positive, as expected (see 5).

There exists an intermediate regime of values of ξ for which the slip distribution changes sign as the slip wave advances. In the current numerical regime, it was found to happen for $\xi \geq 100$. Fig. 7 depicts this situation for $\xi = 150$. As may be seen, the sign of $w(x, t)$ changes as the slip wave progresses, in such a way that the differential displacement between the edge of the contact zone and the region of stick is positive, whilst the slip about the edge of the contact zone is increasingly negative. This is necessary to accommodate the increase in magnitude of the shearing load relative to the frictional one's, which for such ration ξ . The transition is accompanied with a change in sign of $b(x, t)$ (see the inset in Fig. 7); the distribution of dislocations is continuous across this change.

The reverse slip regime is a direct consequence of the kinematic contact condition. If such condition is not observed, and the sign of the frictional force remains negative throughout the contact, inco-

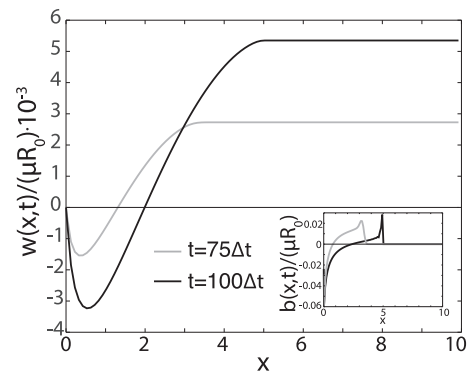


Fig. 7. Magnitude of $w(x, t)$ and (inset) $b(x, t)$ for $\xi = 150$ under a shock load. In this intermediate range, the distribution of slip changes sign midway through the slip wave to accommodate the increase in the shearing load relative to the frictional force.

herent behaviour arises. Such situation is depicted in Fig. 8. A priori, it would seem that the behaviour in this case is not dissimilar from the solutions presented in Figs. 5 and 6, aside from the fact that in this case the sign reversal appears to take place for much smaller values of ξ (and, consequently, larger frictional forces). The problem arises when one considers the meaning of the reverse slip in this case. Here, the sign of the frictional force is always negative, so a negative slip can only be allowed if the sign of the slip velocity is positive. As may be ascertained by comparing Fig. 5a with Fig. 6, this is not the case here: the apparent reverse slip regime arises from the need to accommodate the shearing force alongside a weak frictional force, but rather than allowing the sign of the frictional force reverse its value, here the frictional force is always decreasing the magnitude of the net interfacial force, regardless of

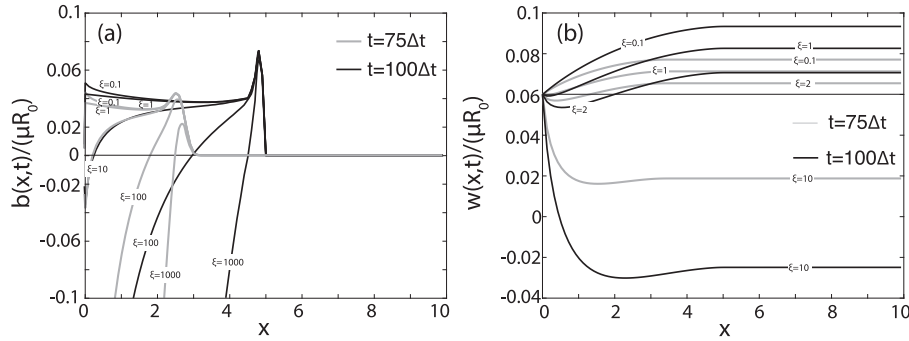


Fig. 8. Magnitude of $b(x, t)$ and $w(x, t)$ for different $\xi = R_0 / (fN_0)$ ratios and a shock load, under the (incorrect) assumption that the sign of the frictional force is always opposite to the shearing force. The same numerical solution parameters as those employed in the frictionless case were used.

the sign of the slip velocity gradient. This also explains why the apparent reverse slip arises in this case for much lower values of ξ (larger values of the frictional force will reduce more the interfacial force), and why the apparent magnitude of the Burgers vector gradient $b(x, t)$ is smaller (the interfacial shear force is weaker because the frictional force is subtracting from the shearing force).

As said, whether the slip reversal will occur is directly related to the relative magnitude between the frictional and shearing loads, which changes over time. We can better understand this if we consider the asymptotic short range solution to Eq. (6.2). Let us therefore expand the kernel $\tau(x - x_0, t - t_0)$ in Eq. (6.2) about $t_0 = 0, x_0 = 0$:

$$\tau(x - x_0, t - t_0) = \frac{\sqrt{t^2 - b^2x^2}}{tx} + O[t_0, x_0] \tag{6.21}$$

Integrating, we find

$$\frac{\sqrt{t^2 - b^2x^2}}{tx} w(x, t) + \text{h.o.t.} = F(x, t) \Rightarrow w(x, t) \approx \frac{tx}{\sqrt{t^2 - b^2x^2}} F(x, t) \tag{6.22}$$

Here $w(x, t) < 0$ entails $|F_{\text{fric}}| < |r(x, t)|$ over short times and short distances. This shows that the transient reverse slip we describe here is related to the relative magnitude of the transient shearing and frictional forces. If the frictional forces are large enough (e.g., in Fig. 5 for $\xi < 100$ under shock loading), the slip reversal does not take place (or else, is observed over very short periods of time). This behaviour is reminiscent of the Adams instability (Adams, 1995, 1998), which occurs as a result of an interfacial resonance along dissimilar materials. As with the Adams instability, it is less likely for larger frictional forces – however, it does not appear to be an inherent surface resonance causing it, but a balance between the shear and frictional forces. It is also reminiscent of the extraneous development of the slip zone reported by Fineberg and coworkers (Ben-David et al., 2010; Ben-David and Fineberg, 2011; Rubinstein et al., 2007, 2004), although in that case it was attributed to a breakdown of the usual frictional law, and not as would happen in this context, due to the interplay between two varying remote loads.

The transient nature of the slip reversal manifest itself in an additional way, in that if sufficient time is allowed to pass, the solution naturally evolves to an expected stick-slip solution. Fig. 9 shows the solution to the shock loaded contact over an extended amount of time. The solution begins as depicted in Fig. 6, as a direct slip solution. Eventually, the magnitude of the shearing force at the edge of the contact zone becomes dominant, and a zone of reverse slip starts to arise about $x = 0$. The solution then evolves in a similar way as that shown in Fig. 8 for $\xi = 150$: the reverse slip peak increases over time, whilst the forward stick magnitude appears to increase. In this case, this mixed reverse-forward slip

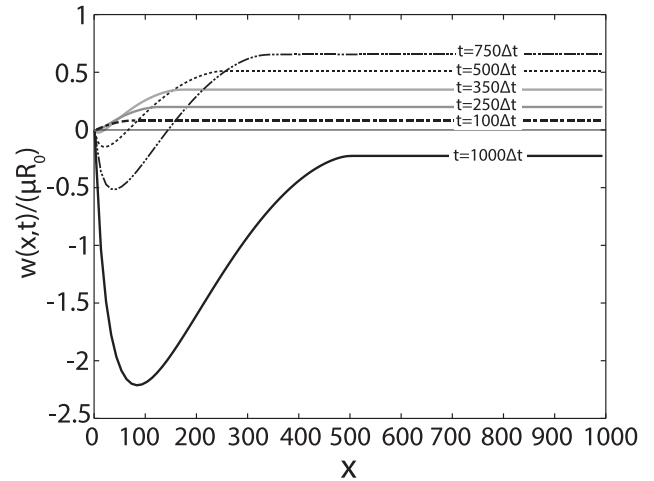


Fig. 9. Magnitude of the relative $w(x, t)$ displacement $\xi = 100$ under shock loading over different instants in time. The solution evolves in time from a fully direct slip wave to a reverse stick-slip wave.

regime peaks at about $t \approx 750\Delta t$. Thereafter, the peak of reverse slip becomes so dominant that the sign of the whole slip distribution is flipped to reverse slip.

The opposite phenomenon, whereby a transient reverse-forward stick-slip wave becomes a fully forwards stick-slip wave, is observed for lower values of ξ . This is particularly clear in the case of a normal ramp loading, where the frictional load increases in magnitude over time, thereby requiring longer times for the solution to evolve from reverse-forward stick-slip wave to a fully reverse (or fully forward) stick-slip wave. Fig. 10 depicts this transient effect that a ramped normal has on the solution; as may be seen, the same regime of forward-reverse stick slip appears to be present; however, in this case the magnitude of the frictional load is ever increasing because the normal load is a ramp, and its increase rate eventually overtakes that of the shearing load irrespective of the value of ξ . This means that in this case eventually all solutions evolve into a fully forward slip ones. Fig. 10 depicts this already happening for $\xi = 10$ in the inset.

The effect of imposing a shearing ramped load (and therefore a ramp friction) rather than a suddenly applied one is also revealing of the transient effects affecting the contact. Because the magnitude of the frictional load increases with $t^{3/2}$, the singularity $1/\sqrt{x}$ at the edge of the contact area is quickly weakened. Thus, the initial magnitude of the friction loads will quickly lose its dominance in leading to the transient forward contact which, as can be seen in Fig. 8 for $\xi = 100$, eventually grows to the reverse contact which we observed in Fig. 6 for $\xi = 100$. In this case, this is brought

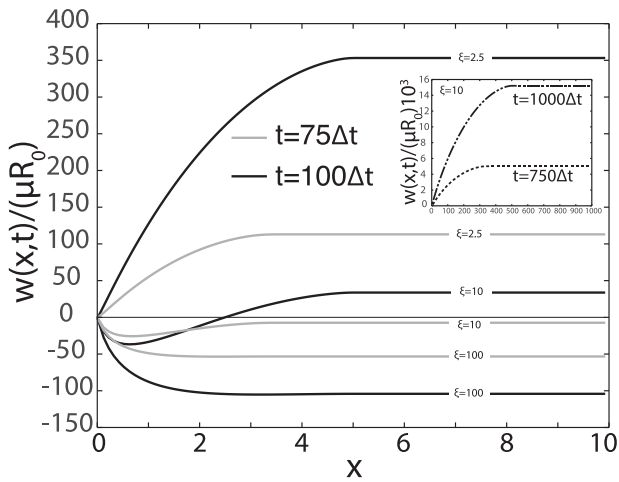


Fig. 10. Magnitude of the relative $w(x, t)$ displacement ξ under normal ramp loading over different instants in time. We note that for $\xi = 10$ the solution changes from fully reverse slip to partial reverse slip to partial forward slip. Over longer periods of time (inset), the solution becomes entirely forward slip.

about by the growth in the magnitude of the shearing load, which being a ramp begins. Thus, an initially slowly varying but subsequently faster growing shearing load such as the ramp load is seen to lead to a transient regime of forward slip that is eventually superseded by a regime of reverse slip. If such sign reversal is to be avoided, it seems that the best strategies are to either decrease lubrication or, else, to impose the external loads in such a way that the shearing load grows at least as fast as the normal load.

Thus, the transient solutions in the presence of friction paint a complicated picture of contact, one where the initiation of the contact is subjected to a regime where partial reverse (or forward) slip of the contact surface may take place, either starting at the edge of the contact zone or within the contact interface. Over time, however, this behaviour recedes and full stick-slip contact is established. Furthermore, and as can be seen in Fig. 11 (and, to a lesser extent, in Fig. 6 for the shock loading case) the transient slip distribution displays large peaks above the relative displacement of the region of stick, i.e., we observe regions of slip where the relative displacement is larger than it is in the region of stick. This is again a transient feature of the solution, and the magnitude of the peaks tend to decrease over time. It is also affected by the magnitude of the frictional forces. For instance, in Fig. 5.b. the relative amplitude of the peak slip for $\xi = 10$ (18% for $t = 75\Delta t$) is clearly smaller than that for $\xi = 2$. (34% for $t = 75\Delta t$); in general, the peak of slip appears to be larger when the frictional forces are weaker.

This study helps understand the nature of the interplay between shearing and frictional forces, and how the interfacial slip

must respond to accommodate it. In general, we find that if the shearing load is larger than the frictional load, then the interfacial slip will tend to evolve to a regime of reverse slip because the shearing force grows faster than the frictional force, and it is of larger magnitude. If the shearing load is close to or weaker than the frictional force, the transient contact interfacial slip will be one of forward (or ‘regular’) slip. This finding appears significant, for in between these two extreme regimes there arises a transitional regime where forward slip may evolve into reverse slip, or vice versa. Because the slip distribution and its sign (and sign reversal) affects the interfacial loads, we expect that such transient regimes will be of importance in the wear performance of the surfaces. It is important to remark that this intermediate regime has been found to appear for values of $\xi \approx 10 - 100$. If the normal and shearing loads are of similar magnitude, this would entail frictional coefficients of $f = 0.1 - 0.01$, which are not unusual (cf. Johnson, 1987).

7. Discussion and conclusions

This article has analysed the transient antiplanar contact between two elastically similar surfaces subjected to dry friction. We have focused solely on the transient problem, i.e., on the nature of the contact problem immediately after contact is established, or after a contact load has changed significantly or significantly fast with respect to its elastostatic value. If the loading is such that it can be divided into a time independent and time dependent part, the transient solution would concern the deviations the time dependent loading induces on the well-known elastostatic solutions (see Barber, 2018; Johnson, 1987).

We have obtained the dynamic loads present in the elastodynamic equivalent to the classical Cattaneo-Midlin problem for a semi-infinite contact, antiplanar interface. Thus, we have employed Kostrov (1966) solution to describe the interfacial shear tractions due to the application of a remote antiplanar shear load. Using a modified version of the Wiener-Hopf technique, we have also rigorously derived the form of the ‘correction’ interfacial shear traction due to a general distribution of slip $w(x, t)$. We have obtained the fundamental solution to this problem, and reached a hypersingular integral describing the stress field dual of $w(x, t)$. We have then employed a convolution argument to modify the integral to a weakly singular form. This form has been found to be a fully elastodynamic extension of Leibfried’s distributed dislocation technique. This approach, not self-similar, may be of further interest in describing elastodynamic problems where an unknown slip distribution results in a balanced stressed field, as could be the case in crack propagation, inclusion expansion, or dislocation pile-ups. The frictional load has been described invoking Amonton’s laws, for which we have employed the quiescent mode I crack’s asymptotic normal traction fields (cf. Freund (1998)).

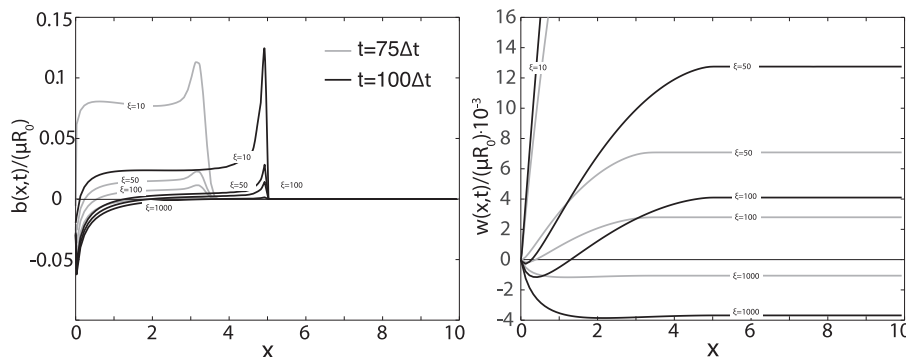


Fig. 11. Magnitude of the relative $w(x, t)$ and $b(x, t)$ when the shearing load is a ramp, and the normal load a shock.

The superposition of shear loading, slip, and friction has led to a bivariate Volterra integral equation, the solution to which is the slip distribution necessary to accommodate the transient loading. This solution can only generally be achieved numerically. A simple Nyström collocation method has then been proposed to solve the said equation, and the main features of the solution have been explored. We have found that the solution invariably consists of a region of slip followed by one of stick. The region of stick is a transient feature, defined by the regions of contact interface that at any instant in time remain unloaded due to the retardation principle affecting the loading. The ensuing slip region is necessary to accommodate the imbalance between the shearing and frictional loads. As in the static case, it tends to grow from the edge of the contact zone inwards; however, in this case it consists of a slip wave that propagates inwards, and that displays a number of relevant transient features.

Crucially, we have found that the transient slip wave can entail a reverse-forward slip regime between the contact surfaces, where the sign of the slip distribution evolves from forward (or regular) slip to reverse slip, i.e., from opposing to having the same nominal sign as the frictional force. This reverse-forward slip wave is brought about by the imbalance between the frictional and shearing loads, and arises when the shearing ones dominate over the frictional ones. It is therefore greater and it lasts longer when the frictional loads are weak. The reverse-forward slip is nonetheless inherently transient, and over time it is observed to lead to either fully reverse slip (particularly for very weak frictional forces), or to fully forward slip (particularly for moderate to large frictional forces). The transient is such that under certain conditions it is possible that what begins as reverse slip evolves into forward slip, or vice versa. The latter appears to occur when the frictional forces are weak (e.g., highly lubricated contact surfaces), whilst the former seems to occur if the frictional coefficient is large. At the same time, the transient slip distribution has been seen to display large peaks above the displacement of the region of stick, i.e., regions of slip where the relative displacement is larger than in the regions of stick, which is not found in the elastostatic case. This peak slip was found to be larger for weaker frictional forces. Thus, there appears to exist a trade-off between avoiding the transient reverse slip by reducing the interfacial friction (for instance, by lubricating it), and minimising the relative magnitude of the slip peak.

We have also explored the importance of the time dependence of the frictional force by considering normal loads other than a shock (or pulse). In studying a ramped application of the frictional force, we have found that this tends to have a stabilising effect over the transient. In general, if the interfacial friction cannot be modified, the best strategy for avoiding transient sign reversals (waves of forward-reverse slip) might be to tune the application of the shearing loads in such a way that they grow at least as fast as a shock load in the near field (i.e., faster than $t^{3/2}$) and faster in the far field.

Much of the nature of the transient contact depends on the form the frictional law takes. In this study we have assumed that Amonton's law with Coulombian friction applies. The role of the kinematic contact condition, whereby the slip velocity must oppose the direction of application of the frictional force, has proven to be crucial in reaching a stable, physically meaningful solution. As we have shown, otherwise one may reach solutions where the slip velocity and the frictional law are of the same sign. Depending on specific applications, it is possible that more complicated models for the interfacial friction such as those based in the Gutenberg–Richter or Omori laws (see Aki and Richards (2002)), may be necessary to better capture the dynamic effects governing the frictional law itself. Future work will explore the influence of frictional laws in the transient response. Alternative kinematic contact conditions based on modern observations of the apparent

breakdown of Amonton's laws under dynamic loading (Ben-David and Fineberg, 2011; Rubinstein et al., 2007) would also affect the solutions presented here.

Although antiplanar contact is of relevance in many industrial applications (e.g., rolling of large cylinders), future work will focus on extending the approach to transient loading presented here to normal contacts, and to contacts between dissimilar materials. We believe that the study of the transient conditions affecting the contact between two surfaces offers a fruitful venue for feature research, and one that is of direct interest to industrial practice. This is because it helps clarify the nature of the contact problem itself under transient loading: we have shown that many transient features, including peaks of slip and loss of contacts, do not manifest in the conventional steady state, nor can be found in the $t \rightarrow \infty$ elastostatic limit. However, many of these features can affect the performance of the contact surfaces and, particularly if they are subjected to cyclic loading, impact the fatigue and wear life of the surfaces. This is particularly true because the transient slip magnitudes can be large, and because these transient features may arise under conditions where the elastostatic solutions expect nothing anomalous.

Acknowledgements

The author duly expresses his gratitude to the Master and Fellows of Trinity College Cambridge for financial support under the author's Title A Fellowship. The author also wishes to thank Prof D Dini for useful comments and discussions.

References

- Abou-Sayed, A.S., Clifton, R.J., Hermann, L., 1976. The oblique-plate impact experiment. *Exp. Mech.* 16 (4), 127–132.
- Achenbach, J.D., 1973. *Wave Propagation in Elastic Solids*. North-Holland, New York.
- Achenbach, J.D., Epstein, H.I., 1967. Dynamic interaction of a layer and a half-space. *J. Eng. Mech.* 93 (5), 27–42.
- Adams, G.G., 1995. Self-excited oscillations of two elastic half-spaces sliding with a constant coefficient of friction. *J. Appl. Mech.* 62 (4), 867–872.
- Adams, G.G., 1998. Dynamic instabilities in the sliding of two layered elastic half-spaces. *J. Tribol.* 120 (2), 289–295.
- Aki, K., Richards, P.G., 2002. *Quantitative Seismology*, second ed. University Science Books, Sausalito, CA.
- Atkinson, K.E., 1997. *The numerical solution of integral equations of the second kind*. Cambridge Monographs on Applied and Computational Mathematics. Cambridge University Press, Cambridge, UK.
- Barber, J.R., 2018. *Contact Mechanics*. Springer, Cham, CH.
- Barsoum, R.S., 1976. On the use of isoparametric finite elements in linear fracture mechanics. *Int. J. Numer. Methods Eng.* 10 (1), 25–37.
- Ben-David, O., Cohen, G., Fineberg, J., 2010. The dynamics of the onset of frictional slip. *Science* 330 (6001), 211–214.
- Ben-David, O., Fineberg, J., 2011. Static friction coefficient is not a material constant. *Phys. Rev. Lett.* 106 (25), 254301.
- Berger, E.J., Begley, M.R., Mahajani, M., 2000. Structural dynamic effects on interface response: formulation and simulation under partial slipping conditions. *J. Appl. Mech.* 67 (4), 785–792.
- Bouchbinder, E., Brener, E.A., Barel, I., Urbakh, M., 2011. Slow cracklike dynamics at the onset of frictional sliding. *Phys. Rev. Lett.* 107 (23), 235501.
- Brock, L.M., 2002. Exact analysis of dynamic sliding indentation at any constant speed on an orthotropic or transversely isotropic half-space. *J. Appl. Mech.* 69 (3), 340–345.
- Brown, J.L., Alexander, C.S., Asay, J.R., Vogler, T.J., Ding, J.L., 2013. Extracting strength from high pressure ramp-release experiments. *J. Appl. Phys.* 114 (22), 223518.
- Brown, J.W., Churchill, R.V., 2009. *Complex Variables and Applications*. McGraw-Hill, Boston, MA.
- Burgers, P., Freund, L.B., 1980. Dynamic growth of an edge crack in a half space. *Int. J. Solids Struct.* 16 (3), 265–274.
- Burgers, P., Freund, L.B., 1981. An addendum to the paper: dynamic growth of an edge crack in a half space. *Int. J. Solids Struct.* 17 (7), 721–727.
- Burridge, R., 1973. Admissible speeds for plane-strain self-similar shear cracks with friction but lacking cohesion. *Geophys. J. Int.* 35 (4), 439–455.
- Burridge, R., Knopoff, L., 1964. Body force equivalents for seismic dislocations. *Bull. Seismol. Soc. Am.* 54 (6), 1875–1888.
- Burridge, R., Knopoff, L., 1967. Model and theoretical seismicity. *Bull. Seismol. Soc. Am.* 57 (3), 341–371.
- Butlin, T., Woodhouse, J., 2009. Sensitivity studies of friction-induced vibration. *Int. J. Veh. Des.* 51 (1–2), 238–257.

- Cagniard, L., 1939. Réflexion et Réfraction des ondes Séismique Progressives. Gauthiers-Villars, Paris.
- Capozza, R., Urbakh, M., 2012. Static friction and the dynamics of interfacial rupture. *Phys. Rev. B* 86 (8), 085430.
- Cattaneo, C., 1938. Sul contatto di due corpi elastici: distribuzione locale degli sforzi. *Rc. Accad. naz. Lincei* 27, 342–348, 434–436, 474–478.
- Colin, J., 2016. Dynamic instability of two elastic half-spaces sliding with a rate-and-state friction constitutive law. *J. Appl. Mech.* 83 (12), 121004.
- Comninou, M., Dundurs, J., 1977. Elastic interface waves involving separation. *J. Appl. Mech.* 44 (2), 222–226.
- Craggs, J.W., Roberts, A.M., 1967. On the motion of a heavy cylinder over the surface of an elastic solid. *J. Appl. Mech.* 34 (1), 207–209.
- De Hoop, A.T., 1960. A modification of cagniard's method for solving seismic pulse problems. *Appl. Sci. Res. B* 8, 349–356.
- Dieterich, J.H., 1972. Time-dependent friction in rocks. *J. Geophys. Res.* 77 (20), 3690–3697.
- Dini, D., Hills, D.A., Solids, J., 2004. Bounded asymptotic solutions for incomplete contacts in partial slip. *Int. Struct.* 41 (24–25), 7049–7062.
- Dini, D., Sackfield, A., Hills, D.A., 2005. Comprehensive bounded asymptotic solutions for incomplete contacts in partial slip. *J. Mech. Phys. Solids* 53 (2), 437–454.
- Doyle, J.F., 1987. Determining the contact force during the transverse impact of plates. *Exp. Mech.* 27 (1), 68–72.
- Duffour, P., Woodhouse, J., 2004. Instability of systems with a frictional point contact. part 2: model extensions. *J. Sound Vib.* 271 (1–2), 391–410.
- Duffour, P., Woodhouse, J., 2007. Instability of systems with a frictional point contact—part 3: experimental tests. *J. Sound Vib.* 304 (1–2), 186–200.
- Eringen, A.C., Suhubi, E.S., 1975. *Elastodynamics*, Volume II. Academic Press, New York.
- Freund, L.B., 1974. The stress intensity factor due to normal impact loading of the faces of a crack. *Int. J. Eng. Sci.* 12, 179–189.
- Freund, L.B., 1998. *Dynamic Fracture Mechanics*. Cambridge Univ. Press, Cambridge, UK.
- Galín, L.A., 1961. Contact Problems in the Theory of Elasticity (trans. H. Moss, I.N. Sneddon). Technical report. North Carolina State Univ., Raleigh, NC.
- Gaul, L., Lenz, J., 1997. Nonlinear dynamics of structures assembled by bolted joints. *Acta Mech.* 125 (1–4), 169–181.
- Gaul, L., Nitsche, R., 2001. The role of friction in mechanical joints. *ASME Appl. Mech. Rev.* 54, 93–110.
- Georgiadis, H.G., Barber, J.R., 1993. On the super-Rayleigh/subseismic elastodynamic indentation problem. *J. Elast.* 31 (3), 141–161.
- Georgiadis, H.G., Charalambakis, N., 1994. An analytical/numerical approach for cracked elastic strips under concentrated loads—transient response. *Int. J. Fract.* 65 (1), 49–61.
- Gurrutxaga-Lerma, B., 2017. Elastodynamic image forces on screw dislocations in the presence of phase boundaries. *Proc. R. Soc. A* 473 (2205), 20170484.
- Gurrutxaga-Lerma, B., 2018. Static and dynamic multipolar field expansions of defects in crystals: dislocations and cracks. *Int. J. Eng. Sci.* 128, 165–186.
- Hansen, P.C., Nagy, J.G., O'Leary, D.P., 2006. Deblurring images: matrices, spectra, and filtering. *SIAM* 3.
- Henshell, R.D., Shaw, K.G., 1975. Crack tip finite elements are unnecessary. *Int. J. Numer. Methods Eng.* 9 (3), 495–507.
- Hills, D.A., Kelly, P.A., Dai, D.N., Korsunsky, A.M., 1996. Solution of crack problems: the distributed dislocation technique. Volume 44 of *Solid Mechanics and its Applications*. Kluwer Academic Publishers, Boston.
- Hills, D.A., Nowell, D., 1994. Mechanics of fretting fatigue. volume 30 of *Solid Mechanics and its Applications*. Kluwer Academic Publishers, Dordrecht, NL.
- Hirani, H., Athre, K., Biswas, S., 1999. Dynamic analysis of engine bearings. *Int. J. Rotating Mach.* 5 (4), 283–293.
- Jaeger, J.C., Cook, N.G.W., Zimmerman, R., 2009. *Fundamentals of Rock Mechanics*. John Wiley & Sons.
- Johnson, K.L., 1987. *Contact Mechanics*. Cambridge Univ. Press, Cambridge, UK.
- Kalker, J.J., 1970. Transient phenomena in two elastic cylinders rolling over each other with dry friction. *J. Appl. Mech.* 37 (3), 677–688.
- Kammer, D.S., Yastrebov, V.A., Spijker, P., Molinari, J.-F., 2012. On the propagation of slip fronts at frictional interfaces. *Tribol. Lett.* 48 (1), 27–32.
- Kawamura, H., Hatano, T., Kato, N., Biswas, S., Chakrabarti, B.K., 2012. Statistical physics of fracture, friction, and earthquakes. *Rev. Modern Phys.* 84 (2), 839.
- Kennett, B.L.N., 1972. The connection between elastodynamic representation theorems and propagator matrices. *Bull. Seismol. Soc. Am.* 62 (4), 973–983.
- Khonsari, M.M., Booser, E.R., 2008. *Applied Tribology: Bearing Design and Lubrication*, 12. John Wiley & Sons.
- Knopp, K., 1996. *Theory of Functions*, Parts I and II. Dover, Mineola, NY.
- Koller, M.G., Bonnet, M., Madariaga, R., 1992. Modelling of dynamical crack propagation using time-domain boundary integral equations. *Wave Motion* 16 (4), 339–366.
- Kostrov, B.V., 1964. Self-similar dynamic problems of the impression of a rigid die in an elastic half-space. *Izv. Akad. Nauk SSSR Mekh. Mashinost.* 4, 54–62.
- Kostrov, B.V., 1966. Unsteady propagation of longitudinal shear cracks. *J. Appl. Math. Mech.* 30 (6), 1241–1248.
- Lapusta, N., Rice, J.R., Ben-Zion, Y., Zheng, G., 2000. Elastodynamic analysis for slow tectonic loading with spontaneous rupture episodes on faults with rate-and state-dependent friction. *J. Geophys. Res.* 105 (B10), 23765–23789.
- Leibfried, G., 1951. Verteilung von versetzungen im statischen gleichgewicht. *Zeitschrift für Physik* 130 (2), 214–226.
- Liu, Y., Rice, J.R., 2005. Aseismic slip transients emerge spontaneously in three-dimensional rate and state modeling of subduction earthquake sequences. *J. Geophys. Res.* 110 (B8).
- Markenscoff, X., 1980. The transient motion of nonuniformly moving dislocations. *J. Elasticity* 10 (2), 193–201.
- Markushevich, A.I., 2005. *Theory of functions of a complex variable*, volume I. American Mathematical Society, Providence, RI, 2nd edition.
- Markushevich, A.I., 2005. *Theory of functions of a complex variable*, volume III. American Mathematical Society, Providence, RI, 2nd edition.
- Martin, P.A., Rizzo, F.J., 1989. On boundary integral equations for crack problems. *Proc. R. Soc. Lond. A* 421 (1861), 341–355.
- Martins, J.A.C., Guimarães, J., Faria, L.O., Vibr, J., 1995. Dynamic surface solutions in linear elasticity and viscoelasticity with frictional boundary conditions. *J. Vib. Acoust.* 117, 445–451.
- Menq, C.H., Griffin, J.H., 1985. A comparison of transient and steady state finite element analyses of the forced response of a frictionally damped beam. *J. Vib. Acoust.* 107 (1), 19–25.
- Meyers, M.A., 1994. *Dynamic Behavior of Materials*. John Wiley, Hoboken, NJ.
- Miklowitz, J., 1978. *The Theory of Elastic Waves and Waveguides*. North-Holland.
- Mindlin, R.D., Appl, J., 1949. Compliance of elastic bodies in contact. *J. Appl. Mech.* 16, 259–268.
- Mura, T., 1982. *Micromechanics of Defects in Solids*, second ed. Kluwer Academic Publishers, Amsterdam.
- Muskhelishvili, N. I., Noordhoff, P., 1953. *Singular integral equations*. Groningen, NL, 2nd edition.
- Nishimura, N., Kobayashi, S., 1989. A regularized boundary integral equation method for elastodynamic crack problems. *Comput. Mech.* 4 (4), 319–328.
- Noble, B., 1958. Methods based on the Wiener-Hopf technique for the solution of partial differential equations. *International Series of Monographs on Pure and Applied Mathematics*, 7. Pergamon Press, New York.
- Nowell, D., Hills, D.A., 1987. Mechanics of fretting fatigue tests. *Int. J. Mech. Sci.* 29 (5), 355–365.
- Nowell, D., Hills, D.A., Sackfield, A., 1988. Contact of dissimilar elastic cylinders under normal and tangential loading. *J. Mech. Phys. Solids* 36 (1), 59–75.
- Pellegrini, Y.P., 2010. Dynamic Peierls-Nabarro equations for elastically isotropic crystals. *Phys. Rev. B* 81, 024101.
- Pellegrini, Y.P., 2014. Equation of motion and subsonic-transonic transitions of rec-tilinear edge dislocations: a collective-variable approach. *Phys. Rev. B* 90 (5), 054120.
- Persson, B.N.J., 2001. Elastic instabilities at a sliding interface. *Phys. Rev. B* 63 (10), 104101.
- Porter, D., Stirling, D.S.G., 1990. *Integral Equations*. Cambridge Univ. Press, Cambridge, UK.
- Ravi-Chandar, K., 2004. *Dynamic Fracture*. Elsevier, Oxford, UK.
- Renardy, M., 1992. Ill-posedness at the boundary for elastic solids sliding under Coulomb friction. *J. Elasticity* 27, 281–287.
- Rice, J.R., 1993. Spatio-temporal complexity of slip on a fault. *J. Geophys. Res.* 98 (B6), 9885–9907.
- Rice, J.R., Ruina, A.L., 1983. Stability of steady frictional slipping. *J. Appl. Mech.* 50 (2), 343–349.
- Rubinstein, S.M., Cohen, G., Fineberg, J., 2004. Detachment fronts and the onset of dynamic friction. *Nature* 430 (7003), 1005.
- Rubinstein, S.M., Cohen, G., Fineberg, J., 2007. Dynamics of precursors to frictional sliding. *Phys. Rev. Lett.* 98 (22), 226103.
- Scholz, C.H., 1998. Earthquakes and friction laws. *Nature* 391 (6662), 37.
- Schwingshackl, C.W., Petrov, E.P., Ewins, D.J., 2012. Effects of contact interface parameters on vibration of turbine bladed disks with underplatform dampers. *J. Eng. Gas Turbines Power* 134 (3), 032507.
- Slepyan, L.I., Brun, M., 2012. Driving forces in moving-contact problems of dynamic elasticity: indentation, wedging and free sliding. *J. Mech. Phys. Solids* 60 (11), 1883–1906.
- Thompson, J.C., Robinson, A.R., 1969. Exact Solutions of Some Dynamic Problems of Indentation and Transient Loadings of an Elastic Half Space. Technical report.
- Tikhonov, A.N., Arsenin, V.Y., 1977. *Methods for Solving Ill-Posed Problems*. John Wiley and Sons, New York.
- Udías, A., 2002. Theoretical seismology: an introduction. In: *International Geophysics*, Vol. 81. Elsevier, pp. 81–102. Chapter 8.
- Vainikko, G., 1993. *Multidimensional Weakly Singular Integral Equations*. Springer, Berlin.
- Verschuere, J., Gurrutxaga-Lerma, B., Balint, D.S., Dini, D., Sutton, A.P., 2017. The injection of a screw dislocation into a crystal: atomistics vs. continuum elastodynamics. *J. Mech. Phys. Solids* 98, 366–389.
- Wayne, V.N., 2000. Brake squeal analysis by finite elements. *Int. J. Veh. Des.* 23 (3–4), 263–275.
- Wiener, N., 1932. Tauberian theorems. *Ann. Math.* 1–100.
- Woodhouse, J., Duffour, P., 2004. Instability of systems with a frictional point contact. Part I: basic modelling. *J. Sound Vib.* 271 (1–2), 365–390.
- Woodhouse, J., Putelat, T., McKay, A., 2015. Are there reliable constitutive laws for dynamic friction? *Philos. Trans. R. Soc. A* 373 (2051), 20140401.